CFA/VISHNO 2016

Self-sustained vortex shedding in a cold-gas scaled model of a large solid rocket motor

L. Hirschberg[a], C. Schram[a] et A. Hirschberg[b]
[a]Von Karman Institute for Fluid Dynamics, Chaussee de Waterloo 72, 1640 Rhode-St-Genese, Belgique
[b]Applied Physics, Technische Universiteit Eindhoven, NT/MTP, CC.3.01b, Postbus 513, 5600MB Eindhoven, Pays-Bas
a.hirschberg@tue.nl

In large scale Solid Rocket Motors flow pulsations can be driven by coupling between vortex shedding and acoustic standing waves in the engine. Cold gas scale model experiments have shown that this process can produce pressure oscillations of the same level as observed in actual full scale engines. Published experiments indicate that when inhibitor rings are used the pulsation level is proportional to the volume of the cavity around the integrated nozzle as used in the Ariane 5 boosters. The air flow in the cold gas scale model is supplied through a porous wall. Using an energy balance approach, an analytical model is proposed in which the system is described as a purely harmonic linearly damped single mode acoustic resonator at a fixed resonance frequency. Losses of acoustic energy due to vortex shedding, acoustic radiation at the nozzle and dissipation in a porous wall are modeled using quasi steady models. Vortex sound theory combined with a simple flow model is used to model acoustic energy production. The model predicts the observed order of magnitude of the pulsation amplitude.

1 Introduction

Solid Rocket Motors (SRMs) as used for Ariane 5 can display strong acoustic pulsations. In the case of these large SRMs the acoustic oscillations can be driven by a coupling between vortex shedding and acoustic standing waves. Anthoine[1] used cold gas scale models to study acoustic oscillations in Solid Rocket Motors. In cold gas experiments combustion of the propellant grain is replaced by injection of air through a porous wall. Most notably Anthoine carried out axial injection experiments in which he found ratios of acoustic pulsation p' to static pressure p of the range $10^{-3} \leq p'/p \leq 10^{-2}$ for flow Mach number $0.05 \leq M \leq 0.15$.

In this communication we will use an energy balance approach in conjunction with the Vortex Sound Theory for an acoustic source model and quasi-steady hydrodynamic models for the acoustic losses to calculate p'/p.

2 Experimental setup

A sketch of the axial injection (1/30) scale model of the Ariane 5 booster as used by Anthoine [1] is shown in Figure 1. Air is injected from a reservoir at a pressure $p_r \simeq 5$ bar, through a porous wall in the head end. The air flows trough a cylindrical pipe, of inner radius r_p and length L_p, which is terminated down stream by an integrated nozzle. The static pressure in the pipe is around $p = 3$ bar. The integrated nozzle has a cavity volume V_c equivalent to the largest cavity volume that occurs during full scale test firing. There are several nozzles which can be mounted corresponding to different cavity volumes. The distance from the bottom of the cavity to the inlet of nozzle measured parallel to the axis is $\delta L_p \simeq 22$mm. The Mach number in the pipe can be varied by reducing the nozzle throat area by the introduction of a needle. The range of the Mach numbers at the nozzle inlet typically considered is $0.05 < M < 0.15$. To simulate an inhibitor, a solid sharp edged orifice of radius r_o is fixed at a distance L_o from the nozzle inlet. This orifice is the vortex generator in the experiments.

A typical result of experiments by Anthoine [1] is shown in Figure 2, for this case $L_p = 0.393$ m, $L_0 = 0.071$ m, $V_c = 2.18 \times 10^{-4}$ m^3 (nozzle 9), $r_p = 0.038$ m and $r_0 = 0.029$ m. In this figure the measured root-mean-square amplitude p_{rms} of the pressure pulsations measured at the head-end normalized with static pressure p_{rms}/p, is shown as a function of the nozzle inlet Mach number M.

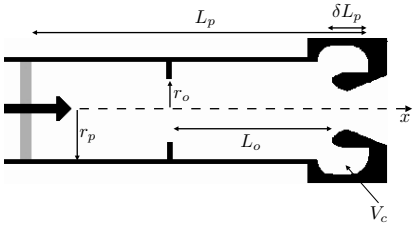

Figure 1: Scale model with axial injection through the upstream porous wall and an integrated nozzle at the downstream side.

3 Theory

An energy balance is proposed to predict the amplitude of the pulsations. Using the fluctuation in total enthalpy $B' = p'/\rho + u'U$ as aeroacoustic variable for $M^2 << 1$ allows to take convective effects in the boundary conditions while neglecting these in the bulk of the acoustic field [7]. The total enthalpy is related to the velocity fluctuation u' by the linearized Euler equation $\partial u'/\partial t = -\partial B'/\partial x$. Assuming a stable limit cycle, the acoustic field is approximated by a single mode n of a close-close pipe of effective length $L_{eff} = L_p - \delta L_p + V_c/(\pi r_p^2)$:

$$B' = |b| \cos(\frac{\omega_n}{c} x) \cos(\omega t) \tag{1}$$

with $|b|$ the amplitude of B' at an anti-node, $\omega_n = n\pi c/L_{eff}$, c the speed of sound, x the distance from the upstream end of the pipe and ω the oscillation frequency. As proposed by Culick [2] the system is described as a damped oscillator:

$$M_{eff} \frac{d^2 b}{dt^2} + \gamma_{eff} \frac{db}{dt} + M_{eff} \omega_n^2 b = F_{vortex} \tag{2}$$

where $M_{eff} = \rho \pi r_p^2 L_{eff}/(\omega_n c)^2$. The linear damping γ_{eff} is de sum of nozzle radiation, vortex shedding at the orifice and viscous damping in the porous end-wall. Using quasi-steady models one obtains [5]:

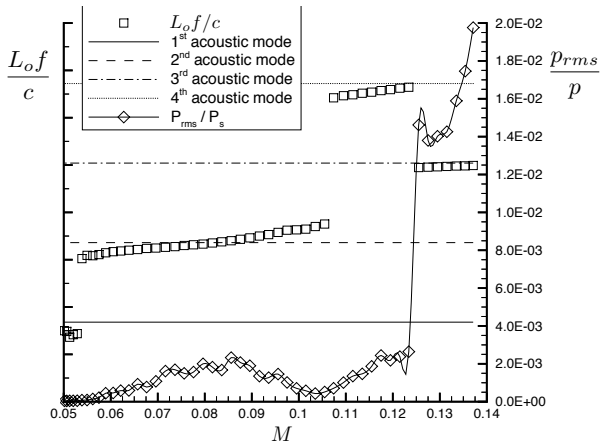

Figure 2: Anthoine's experimental results for $L_p = 0.393$ m, $r_0 = 0.029$ m, $L_o = 0.071$ m and $V_c = 2.18 \times 10^{-4}$ m^3 (nozzle 9). The pulsation amplitude is indicated using a diamond and the corresponding frequency by a square. On the righthand vertical axis we have pulsation levels p_{rms}/p and on the lefthand vertical axis the oscillation frequency $L_o f/c$ both as a function of the Mach number M. The horizontal lines indicate the resonance frequencies which Anthoine [1] calculates as follows: $f_n = nc/(2L_p)$ with $n = 1, 2, 3 \ldots$. Typical pulsation levels reach $O(10^{-2})$ and the oscillation frequency increases monotonously for each acoustic mode, passing the resonance frequency around the maximum pulsation level.

$$\begin{aligned} \gamma_{eff} &= \frac{\rho\pi r_p^2}{\omega^2 c}[1 - R_{nozzle}^2\left(\frac{1-M}{1+M}\right)^2 \\ &+ \frac{\omega_n}{\omega}M\left(\left(\frac{r_p}{r_{jet}}\right)^4 - 1\right)\sin^2(\frac{\omega_n}{c}x_o) \\ &+ 1 - R_{porous}^2\left(\frac{1+M}{1-M}\right)^2] \end{aligned} \quad (3)$$

The pressure reflection coefficient at the nozzle R_{nozzle} is given by the theory of Marble and Candel [6] $R_{nozzle} = (1 - \frac{\gamma-1}{2}M)/(1 + \frac{\gamma-1}{2}M)$ where γ is the Poisson ratio of specific heats. The pressure reflection coefficient R_{porous} end-wall is given by [5]: $R_{porous} = (1 + (p_r/p)^2(\gamma M - 1))/(1 - (p_r/p)^2(\gamma M - 1))$ where p_r is the reservoir pressure upstream of the porous wall and p the time averaged pressure in the pipe. The power generated by the vortex sound source term F_{vortex} is calculated using the energy corollary of Howe [4]:

$$< F_{vortex}\frac{db}{dt} >= -\rho < \int_V (\vec{\omega} \times \vec{v}) \cdot \vec{u}_{ac} dV > \quad (4)$$

where $\vec{v}$ is the local velocity field and $\vec{u}_{ac}$ is the unsteady potential flow component of the velocity identified by Howe [4] as the acoustic field. The brackets $< \ldots >$ indicate time averaging over a period of oscillation and the integral is carried out over the volume in which the vorticity $\vec{\omega} = \nabla \times \vec{v}$ is non vanishing. The vorticity field is described in terms of line vortex rings of circulation Γ convected at constant speed $u_\Gamma = 0.4U(r_p/r_{jet})^2$:

$$\vec{\omega} = \Gamma\delta(r - r_{jet})\delta(x - x_o - u_\Gamma(t - \tau_0)). \quad (5)$$

Assuming quasi-steady shedding of vorticity followed by the concentration of this vorticity each period into a single vortex, the circulation is given by: $\Gamma = (\pi/\omega)[U(r_p/r_{jet})^2]^2$ where the vena contracta ratio r_{jet}/r_o of the jet cross-sectional radius r_{jet} and orifice radius r_o is determined from the experimental data of Gilbrag [3]. The acoustic field $\vec{u}_{ac}$ is assumed to have a uniform component v_{ac} normal to $\vec{\omega}$ and $\vec{v}$ over a distance L_c upstream from the nozzle inlet $x = L_p - \delta L_p$:

$$\begin{aligned} v_{ac} &= \frac{r_p|b|\omega_n}{2cL_c\omega}\sin(\frac{\omega_n}{c}(L_p - \delta L_p))\sin(\omega t) \\ &\times [H(x - (L_p - \delta L_p - L_c)) \\ &- H(x - (L_p - \delta L_p))] \end{aligned} \quad (6)$$

The distance L_c was estimated as $L_c = 2\sqrt{2}(r_p - r_n)$ where $r_n = 1.85$ cm is the nozzle radius at the minimum of the cavity inlet. Substitution in the energy corollary (4) yields:

$$\begin{aligned} < F_{vortex}\frac{db}{dt} > &= \\ \frac{\pi\rho\Gamma r_{jet}u_\Gamma r_p\omega_n}{cL_c\omega} &|b| \sin(\frac{\omega_n}{c}L_p) \\ \times < \sin(\omega t)[H(t - \tau_0 - \frac{L_o - L_c}{u_\Gamma}) &- \\ H(t - \tau_0 &- \frac{L_0}{u_\Gamma})] > \end{aligned} \quad (7)$$

where $L_o = L_p - \delta L_p - x_o$ is the distance between the orifice and the nozzle inlet and $\tau_0 = 0$ or π/ω depending on the position x_o of the orifice relative to pressure nodes. The parameter τ_0 is chosen such that a new vortex is shed each time the acoustic velocity vanishes at the orifice turning into the direction of the main flow U. The amplitude $|b|$ is obtained from the energy balance:

$$< F_{vortex}\frac{db}{dt} >=< \gamma_{eff}\left(\frac{db}{dt}\right)^2 > \quad (8)$$

in which we use the approximation $\omega = \omega_n$.

4 Results

In Figure 3 results of the energy balance are compared to axial cold flow experiments for nozzle 9 with $V_c = 2.18 \times 10^{-4}$ m^3. The results of the energy balance prediction are shown in the plot on the lefthand side of Figure 3. The ratio of root mean square value of the pressure fluctuation over the static pressure p_{rms}/p is plotted as a function of the Mach number M. This is done for three cases viz. where the frequencies equal the resonance frequencies ω_1, ω_2 and ω_3 corresponding to the first $n = 1$ (dotted line) second $n = 2$ (solid line) and third $n = 3$ (dashed line) acoustic mode respectively.

For comparison the results of the experiments as published by Anthoine[1] are displayed on the righthand side in Figure 3. On the lefthand vertical axis the dimensionless frequency $L_o f/c$ is shown and on the righthand vertical axis the p_{rms}/p, both as a function of the Mach number M. From the Figure 3 we see that local maxima in relative pulsation amplitude p_{rms}/p are detected around $M = 0.085$ and $M = 0.14$. As we can see from Figure 3, these correspond to the second $n = 2$ and third $n = 3$ acoustic mode respectively.

The local maxima measured at around $M = 0.085$ and $M = 0.14$ respectively correspond to a hydrodynamic number $m = L_o f/u_\Gamma = 2.0$. The hydrodynamic number is the ratio of the convection time of the vortex from the orifice to the nozzle inlet and the oscillation period. I.e. it is a estimate of the number of equidistant vortices traveling from the orifice to the nozzle. Moreover, for $m = 1, 2, 3$ we speak of the first second and third hydrodynamic mode. For $M = 0.085$ the first, second and third hydrodynamic modes correspond to the first $n = 1$, second $n = 2$ and third $n = 3$ acoustic modes respectively. While for $M = 0.14$ the second and third hydrodynamic modes correspond to the first $n = 1$ and second $n = 2$ acoustic modes respectively. It is noteworthy that in simulations with $M = 0.09$ Anthoine[1] finds two vortices traveling down steam viz. the second hydrodynamic mode. This would explain the selection of the second acoustic mode $(m, n) = (2, 2)$ at $M = 0.085$ and the selection of $(m, n) = (2, 3)$ for $M = 0.14$.

We now concentrate on the second acoustic mode $n = 2$. However the procedure described can equally be applied to third mode $n = 3$. To compare the experimental data to the energy balance we do the following: locate the local maximum for $n = 2$ in the experiments. This yields a measured relative pressure pulsation $(p_{rms}/p)_{exp} = 2.3 \times 10^{-3}$ with an associated Mach number $M_{exp} = 8.6 \times 10^{-2}$. We now turn to the plot of the energy balance on the lefthand side of Figure 3. As we are concerned with the second acoustic mode $n = 2$, we focus on the solid line. We find the local maximum closest to the one detected by Anthoine[1], which is $(p_{rms}/p)_{th} = 7.5 \times 10^{-3}$ with a corresponding Mach number $M_{th} = 8.5 \times 10^{-2}$. Thus in this case we accurately reproduce the corresponding Mach number within 1%. And the pulsation amplitude p_{rms}/p is calculated using the energy balance method is a factor 3 higher than what was measured.

The results depicted in Table 1 correspond to experiments for nozzle 7 with $V_c = 1.84 \times 10^{-4}$ m^3 in which the length of the test section L_p was varied. The local maxima in p_{rms}/p for the experiments (column 4) and the energy balance prediction (column 6) are compared (column 7). We have scaled the maxima in p_{rms}/p in Table 1 using the associated dynamic pressure i.e. $\rho u^2/2 = \gamma p M^2$. From the this table we see that using the energy balance approach, we can reproduce the measured pressure pulsations within and order of magnitude. Furthermore, we see that pulsations are of the order magnitude of the dynamical pressure i.e. $\frac{1}{2}\rho U^2 = \gamma p M^2$ can be used as an order of magnitude estimate for pressure amplitude of the pulsations.

In a companion paper we discuss a more detailed model which predicts the evolution of the frequency ω as a function of the Mach number M [5]. The present simpler energy balance approach appears to be more robust and does provide similar results for the pulsation amplitude.

5 Conclusion

In this communication we analyzed results of axial injection cold flow experiments, carried out using a (1/30) scale model for Ariane 5. We have shown that the energy balance method can reproduce measured maxima in pressure pulsation p_{rms}/p within a factor 6 and its associated Mach number M within 10%, when the oscillating mode number observed in the experiments is used as an input parameter. Its is thusly useful as a tool for interpreting measurements viz. the physical models for the source and the losses provide qualitative insight into the occurrence of dominant physical processes. What is more, we have shown that the dynamical pressure $\frac{1}{2}\rho U^2$ is a good order of magnitude estimate for typical maxima of pressure pulsations.

Acknowledgements

Support by Airbus Defense and Space and in particular Jean Collinet and Serge Radulovic is acknowledged.

References

[1] J. Anthoine, *Experimental and numerical study of aeroacoustic phenomena in large solid propellant boosters with application to Ariane 5 solid rocket motor*, von Karman Institute for Fluid Dynamics, Sint-Genesius-Rode, Belgium (2000)

[2] F. E. C. Culick, *Unsteady Motions in Combustion Chambers for Propulsion Systems*, RTO/NATO, RTO-AG-AVT-039 (2006)

[3] D. Gilbrag, *Handbuch der Physik: Strömungsmechanik III*, Springer-Verlag, (1960).

[4] M. S. Howe, The dissipation of sound at an edge, *Journal of Sound and Vibration* **3**, 407-411 (1980).

[5] L. Hirschberg, C. Schram , A. Hirschberg, Prediction of pulsations in a cold-gas scale-model of a solid rocket motor, *proceeding for 22nd AIAA/CEAS*, Lyon (2016).

[6] F. E. Marble, S. M. Candel, Acoustic disturbance from gas non-uniformities convected through a nozzle, *Journal of Sound and Vibration* **2**, 225-243 (1977).

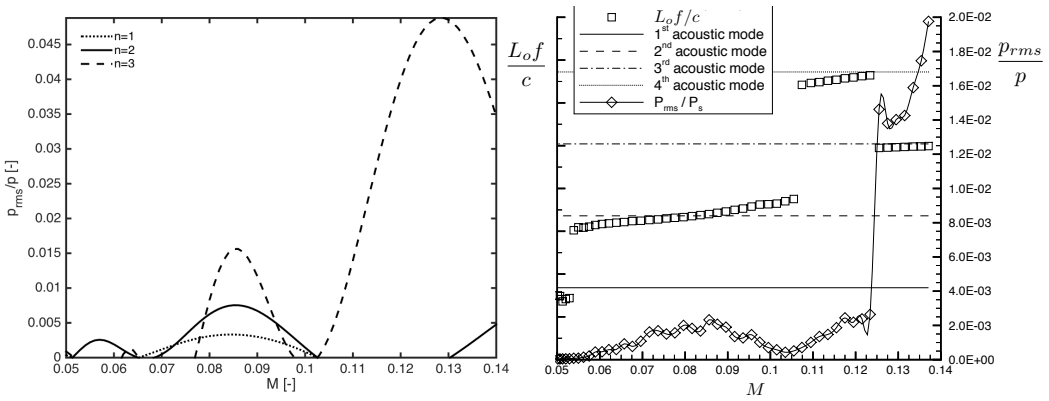

Figure 3: On the lefthand side the relative pulsations, for the first $n = 1$ (dotted line), second $n = 2$ (solid line) and third $n = 3$ (dashed line) acoustic modes, predicted by the energy balance are plotted as a function of the Mach number at the nozzle inlet. Anthoine's experimental results are shown on the righthand side for comparison ($L_p = 0.393$ m, $r_0 = 0.029$ m, $L_o = 0.071$ m). The pulsation amplitude is indicated using a diamond and the corresponding frequency by a square. On the righthand vertical axis we have pulsation levels p_{rms}/p and on the lefthand vertical axis the oscillation frequency $L_o f/c$ both as a function of the Mach number M. The horizontal lines indicate the resonance frequencies which Anthoine [1] calculates as follows: $f_n = nc/(2L_p)$ with $n = 1, 2, 3 \ldots$. Typical pulsation levels reach $O(10^{-2})$ and the oscillation frequency increases monotonously for each acoustic mode, passing the resonance frequency around the maximum pulsation level.

Table 1: Results for variable tube length L_p. The first five columns contain data taken from Anthoine's cold flow experiments [1]. The last two columns list the theoretical predictions, obtain with the energy balance ($L_o = 7.1 \times 10^{-2}\, m$, $r_o = 2.9 \times 10^{-2}\, m$, $\left(\frac{r_{jet}}{r_p}\right)^2 = 0.68$). In columns 4 and 6 the maxima in p_{rms} for the experiments and the energy balance prediction are scaled using the associated dynamic pressure i.e. $\rho u^2/2 = \gamma p M^2$

m	n	L_p	M_{exp}	$\left(\frac{2p_{rms}}{\gamma p M^2}\right)_{exp}$	M_{th}	$\left(\frac{2p_{rms}}{\gamma p M^2}\right)_{th}$	$\frac{p'_{th}}{p'_{exp}}$
[−]	[−]	$[m] \times 10^{-1}$	$[-] \times 10^{-2}$	[−]	$[-] \times 10^{-2}$	[−]	[-]
2	2	3.93	8.0	0.44	8.7	1.4	3.2
2	3	3.93	14	0.68	13.1	3.3	4.8
4	2	3.05	6.0	0.08	5.5	0.19	2.5
2	2	3.05	11	0.44	11.1	1.1	2.6
4	1	1.88	7.8	0.31	8.7	1.5	4.8
3	2	1.88	12	0.44	12.6	0.85	2.0
4	1	1.63	9.8	0.24	9.9	15	6.3

[7] F. Nicoud, K. Wieczorek, About the zero Mach number assumption in the calculation of thermoacoustic instabilities, *International Journal of Spray and Combustion Dynamics* **1**, 67-111 (2009).